Oxidation behaviour of nanostructured Ti-B-N based coatings

M. Cabibbo, S. Spigarelli

Nanostructured Ti-B-N based coatings are widely employed in many applications for the excellent properties such as high hardness, low friction, good resistance to wear and corrosion. In addition, if some alloying elements such Al and Si are incorporated an oxidation improved resistance is achieved. In the present work, Ti-B-N, Ti-Si-B-N and Ti-Al-Si-B-N coatings deposited by Ion Implantation Assisted Magnetron Sputtering (IIAMS) have been investigated. All the coatings were deposited on single-crystal Si-[100]. To evaluate the oxidation behavior, the coatings were annealed in air at 700 and 900°C for 4 hours. Ti-B-N coatings oxidizes completely after annealing at 700°C for 4 hours, while a layered structure with well-definite interface is produced on Ti-Si-B-N and Ti-Al-Si-B-N based coatings. Upon annealing at 900°C, the Si-doped film showed significantly better oxidation resistance compared to that of Ti-B-N and Ti-Al-Si-B-N coatings.

INTRODUCTION

In the last years, Ti-nitride based coatings have been widely employed in several industrial applications because of their superior mechanical properties [1-3]. However, another important characteristic of such coatings is the stability of their mechanical properties at elevated temperatures. In fact, thermal stability and oxidation resistance of Ti-N based coatings have been extensively investigated in order to prevent the degradation of their mechanical and tribologic properties at high working temperatures. In many works, it is reported that an improvement of the mechanical properties of Ti-N coatings is achieved by including B into the film, whereas additives elements such as Si, Al, Cr, provide a better thermal stability against oxidation [3-12]. Recently, Kiryukhantes-Korneev et al. [6] studied the oxidation behaviour of Ti-B-N based coating up to 900°C for 1 h. Those results showed poor oxidation resistance upon the tested experimental conditions. Since the coated components could be subjected to high temperature for longer period of time during their service life time, the present work reports a comparison of the oxidation behaviour of Ti-B-N, Ti-Si-B-N and Ti-Al-Si-B-N coatings after annealing treatments at 700°C and 900°C for 4 h. The Al and Si incorporation effects on the microstructure and composition evolution of the Ti-B-N coatings with the annealing temperature were studied by Atomic Force Microscopy (AFM), X-Ray Diffraction (XRD) and Transmission Electron Microscopy (TEM).

EXPERIMENTAL DETAILS

Ti-B-N based coatings were produced in the Moscow State Institute of Steel and Alloys (MSISA). The coatings were deposited on single-crystal Si [100] using IIAMS apparatus in a gaseous mixture of $Ar + N_2$. The total pressure in the chamber was maintained at 0.01 Pa and the partial pressure of N_2 was of 15% of the total one. The distance between targets and substrates was ~ 100 mm. The applied bias voltage was kept to ~ - 250 V and the discharge magnetic current was 2.3 A. In order to remove oxides and impurity atoms on the surface, substrates were ion etched by Argon beam with energy of 1.5 KeV for 10 minutes before deposition. During the deposition process, the substrate temperature was 280°C and the deposition time was set to achieve a film thickness of approximately 2 μm.

Isothermal annealing was performed at 700° and 900 °C for 4 h in air and the samples were left to cool at room temperature after thermal treatments.

Surface morphology of as-deposited and annealed films were observed by Metris-2001 Burghler Instrument® AFM used in contact mode. Phase composition and microstructure were investigated by X-Ray Diffractometer (D5000, Siemens®) operating at 40 kV and 30 mÅ, with Cu Kα radiation ($\lambda_{Cu} K_\alpha$ = 0.154 nm) and a Philips® CM 200 TEM operating at 200 kV.

For TEM observations, the as-deposited and air annealed coatings were prepared by cross-section method gluing face-to-face two portions of same sample. Afterwards, the 'sandwiches' were cut in 500 m thick cross-section slides and abraded to ~ 100 μm thickness. The slides were polished to obtain a mirror-like surface finishing and 3-mm disks were extracted using an ultrasonic cutter. An additional mechanical grinding was carried out by dimpling the central part of the 3-mm disks up to a thickness of approximately 15 μm. Finally, the samples were mechanically thinned to the hole using a low-angle ion milling system (Gatan® Precise Ion Polish System) with beam angle inclination to the sample surface starting at 8° and ending at 2° under a constant voltage of 4 KeV.

RESULTS & DISCUSSION

The chemical composition of the coatings were measured by glow discharge optical spectroscopy (GDOS) and the results are reported in Table 1. It was found that a certain amount of Ar and impurities such as C and O (not reported in Tab.1) were incorporated into the coatings during the deposition process; anyway, their content was lower than 4 at.%. Figure 1 shows XRD θ-2 re-

M. Cabibbo, S. Spigarelli
V.I.N.F (Virtual Institute of NanoFilms), web site: www.vinf.eu)
Dipartimento di Meccanica, Università Politecnica delle Marche,
Via Brecce Bianche, 60131, Ancona, Italy.
Corresponding author: prof. Marcello Cabibbo,
Email: m.cabibbo@univpm.it, Fax: 0712204801

Coating	Elemental Composition (at %)				
	Ti	B	N	Si	Al
Ti-B-N	46	31	23	-	-
Ti-Si-B-N	22	43	14	21	-
Ti-Al-Si-B-N	31	25	28	10	6

TAB. 1 *Atomic concentration of Ti-B-N based coatings.*

Percentuale atomico dei rivestimenti a base Ti-B-N.

FIG. 1 *XRD spectra of the as-deposited Ti-B-N, Ti-Si-B-N and Ti-Al-Si-B-N coatings.*

Spettri XRD dei rivestimenti come depositati, Ti-B-N, Ti-Si-B-N e Ti-Al-Si-B-N.

corded patterns of the as-deposited coatings. The Ti-B-N coating showed broad peaks which are consistent with the cubic NaCl-type structure of TiN. As the coating is doped with Si, XRD spectrum displays two broad peaks at about 34° and 43.6° consistent respectively with the peaks (100) and (101) of the TiB_2 phase. Furthermore, the peak intensities of Ti-Si-B-N coatings are lower than the Ti-B-N ones. For Ti-Al-Si-B-N coating, only sharp peaks due to impurities in the film appear, indicating the presence of large fractions of amorphous phase. Thus, XRD inspections revealed an amorphous structure generated by the addition of Si
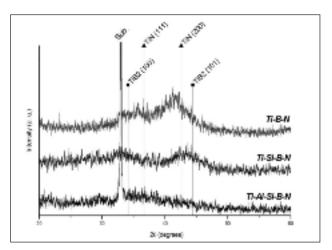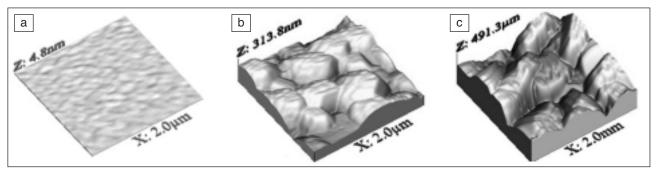

FIG. 2 *AFM images of Ti-B-N coating a) in as-deposited conditions and after annealing at b) 700°C and c) 900°C.*

Immagini AFM del rivestimento Ti-B-N a) come depositato; b) dopo trattamento a 700°C/4h; c) dopo trattamento a 900°C/4h.
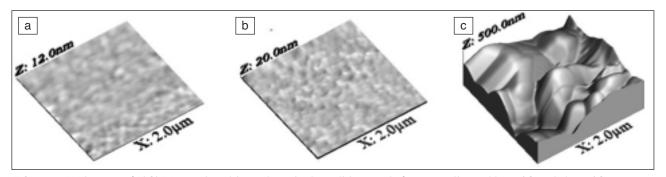

FIG. 3 *AFM images of Ti-Si-B-N coating a) in as-deposited conditions and after annealing at b) 700°C and c) 900°C.*

Immagini AFM del rivestimento Ti-Si-B-N a) come depositato; b) dopo trattamento a 700°C/4h; c) dopo trattamento a 900°C/4h.
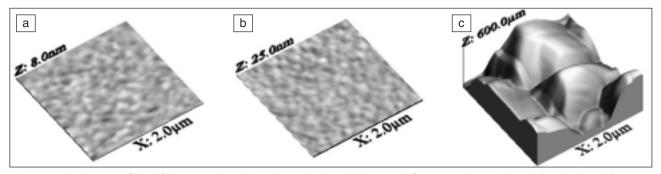

Fig. 4 *AFM images of Ti-Al-Si-B-N coating a) in as-deposited conditions and after annealing at b) 700°C and c) 900°C.*

Immagini AFM del rivestimento Ti-Al-Si-B-N a) come depositato; b) dopo trattamento a 700°C/4h; c) dopo trattamento a 900°C/4h.
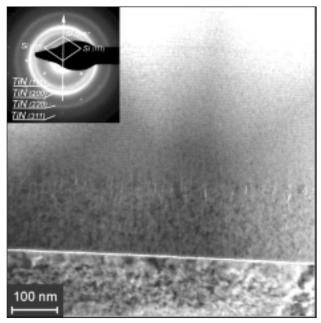
FIG. 5 *Cross-section TEM image of the as-deposited Ti-B-N coating with corresponding SAED pattern.*

Immagine TEM e relativa SAEDP di una cross-section del rivestimento Ti-B-N.

and Al to the Ti-B-N coating. The evolution of surface morphologies of Ti-B-N based coatings was investigated by AFM in contact mode. Figures 2, 3 and 4 reports the AFM 2 x 2 m^2 images of the surface morphology of the as-deposited and annealed coatings. The surface morphologies of the as-deposited coatings (Figs. 2a, 3a and 4a) were homogenous and characterized by a very fine granular structure. Additionally, their roughness values are similar to the typical roughness of the polished Si substrate (~ 1.0 nm) indicating a very smooth coating surfaces.

After the 700°C annealing, the morphology of the Ti-B-N coating changes drastically because of the growth of oxide crystallites (Fig. 2b) while no significant topography modifications were detected in the Ti-B-N based coatings (Figs. 3b and 4b). Typical surface morphologies of annealed coatings at 900°C are showed in Figs. 2c, 3c and 4c. With increasing annealing temperature up to 900°C, the Ti-B-N film does not reveal further morphology variations, suggesting an oxidation phenomenon saturation which had already reached at 700°C. On the other hand, the oxidation phenomena, occurred at 900°C, completely jeopardized the surface integrity of the coating. The roughness and morphology of doped Ti-B-N coatings showed the formation of coarse oxide crystallites.

Morphology inspections of the Ti-B-N based coatings after annealing at 700 and 900°C showed a better oxidation resistance than that of the Ti-B-N. Anyway, deeper characterization of the as-deposited and annealed coatings was performed by TEM on cross section samples.

Figure 5 reports a cross-section TEM micrograph of the as-deposited Ti-B-N coating on Si substrate. The coating shows a well-defined multilayered structure with a layer period of about 5/10 nm. Additionally, a nano-grained layer of approximately 150 nm in thickness is formed above the Si substrate. The selected area electron diffraction (SAED) patterns recorded from the multilayer zone and the nanometric grained layer overlapped: they present three continuous diffraction rings, implying a random orientation of crystallites, and a cubic B1 NaCl-type structure. The lattice parameters related to the cubic planes (111), (200), (220) and (311) were identified as TiN. Intensity of the rings confirmed a well developed (111) and (200) texture components. It is worth to notice that the intensity of the (200) ring is not uniform and the position of the intensity maxima are consistent with the development of a preferential orientation parallel to the (100)-Si reflection. These results are in good agreements with XRD measurements.

The Ti-Si-B-N based coatings show a more evident dense and amorphous-like structure (Figs 6a and 6b). The SAED pattern of Ti-Si-B-N is constituted by continuous rings with uniform intensity revealing a fine scale, randomly oriented, polycrystalline microstructure. The coating shows an hexagonal close-packed (hcp) AlB_2 - type structure without texture. By indexing the diffraction pattern, it results that it is constituted by TiB_2 phase, as XRD measurements have also shown. The SAED pattern corresponding to the Ti-Al-Si-B-N coating showed quite broad diffraction rings with low intensity, suggesting a superposition of crystalline and amorphous phase (fig. 6b). Nevertheless, the
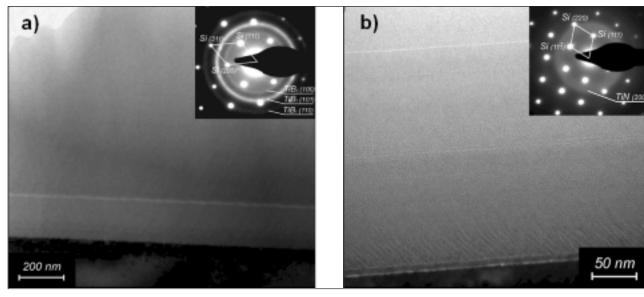

FIG. 6 *Cross-section TEM images of the a) Ti-Si-B-N and b) Ti-Al-Si-B-N coatings with related SAED patterns.*

Immagine TEM e relativa SAEDP di una cross-section dei rivestimento a) Ti-Si-B-N e b) Ti-Al-Si-B-N.
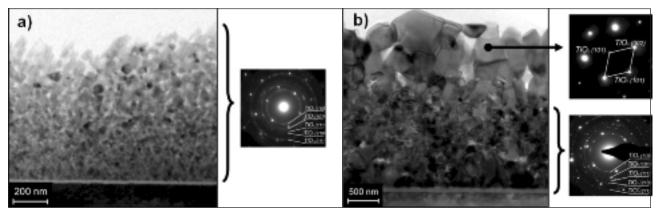
FIG. 7   *TEM micrograph of the Ti-B-N coating after a) annealing at 700°C/4h and b) annealing at 900°C/4h.*

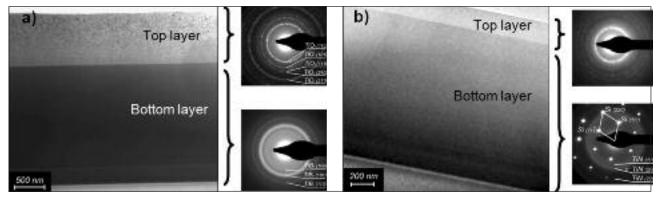*Micrografie TEM del rivestimento Ti-B-N a) dopo esposizione a 700°C/4h e b) a 900°C/4h.*

FIG. 8   *Cross-section TEM micrographs of a) Ti-Si-B-N and b) Ti-Al-Si-B-N coatings after annealing at 700°C.*

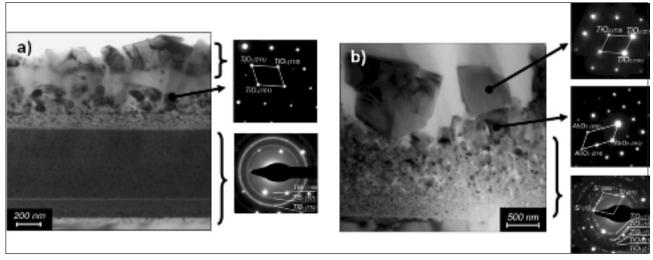*Micrografie TEM di rivestimenti a) Ti-Si-B-N e b) Ti-Al-Si-B-N sottoposti a 700°C/4h.*

FIG. 9   *Cross-section TEM micrographs of a) Ti-Si-B-N and b) Ti-Al-Si-B-N coatings after annealing at 900°C/4h.*

Micrografie TEM dei rivestimenti a) Ti-Si-B-N e b) Ti-Al-Si-B-N sottoposti a 900°C/4h.

broad diffraction ring and their low intensity make difficult the unambiguous determination of the lattice parameters.
The corresponding d-spacing is in the range of 2.09 - 2.17 Å. Therefore, the diffraction ring could be attributed to the (200) more intense peak of TiN phase.
The cross-section of the Ti-B-N coating annealed at 700°C shows clearly a nanostructure morphology (Fig. 7a). The average grain size progressively decreased from 150 to 20 nm increasing the distance from the coating surface.

The formation of sub-micrometer crystallites on the coating surface modifies drastically the morphology of the as-deposited coating, as confirmed by the AFM observations (Fig. 2). The corresponding SAED pattern showed an evident ring-like diffraction pattern consistent with rutile-TiO_2 oxide crystallites, indicating a complete coating oxidation after 4h at 700°C.
Figure 7b shows the Ti-B-N cross-section microstructure after 4h at 900°C. The annealed coating is composed by coarse crystallites on the top of the film, as observed by AFM (Fig.2c). The

corresponding SAED diffraction pattern resulted in single crystal pattern, which was indexed as rutile-TiO_2 phase.

The region beneath was characterized by finer crystallites with average size of ~ 100 nm, and a quasi continuous ring-like diffraction pattern corresponding to TiO_2 phase. Thus, also the annealing treatment at 900°C caused a complete coating oxidation and promoted the recrystallization of the TiO_2 crystallites in the bottom layer.

Figure 8 reports cross-section TEM micrographs of the Ti-Si-B-N and Ti-Al-Si-B-N coatings after annealing at 700°C. The oxidation treatment produced a well-defined two-layer structure in both coatings. The top layers, 800 and 200 nm-thick, respectively for Ti-Si-B-N and Ti-Al-Si-B-N, are constituted by very fine nano-crystallites which do not compromise the coating surface morphology as also reported in Figs. 3b and 4b.

In the Ti-Si-B-N coating, the average crystal size is ~ 20 nm on the coating surface and decreases to few nanometers in the top/bottom layers interface. By indexing the corresponding SAED pattern, it resulted that the top layer is composed by nano-crystallites of rutile-TiO_2 phase. Conversely, the morphology of the bottom layer indicated an amorphous-like structure and the corresponding SAED pattern is consistent with the same TiB_2 phase. This means that the oxide top layer acts as a protective barrier preventing a longer oxidation in the Ti-Si-B-N coating.

The Ti-Al-Si-B-N coating annealed at 700°C/4h, the 200 nm-thick top layer is constituted by nano-crystallites with an average size of ~ 5 nm. The related SAED pattern is indexed in accordance with AlyTixSiOz phase (JCPDS card No. 22-0502). The formation of Al-Ti-Si rich oxide phase is also reported in [6]. The bottom layer morphology showed an amorphous-like structure and the diffraction pattern is consistent with the TiN phase. At 700°C, the oxidation mechanism consists in the oxygen diffusion into the coating, while Ti, Si, and Al from the coatings diffuse outward, thus forming the oxidized layer.

In the Ti-Si-B-N coating, a partial oxidation is achieved due to the oxide layer formation of a protective barrier, which limits the inward oxygen diffusion. Moreover, such coating showed a better oxidation resistance than the Ti-Si-B-N because of the smaller thickness of the oxide top layer. These results are in good agreement with the Kiryukhantes-Korneev et al. [6] findings.

The TEM micrographs of the Ti-Si-B-N and Ti-Al-Si-B-N coatings after annealing at 900°C are reported in Fig. 9. Due to the formation of coarse crystallites on the coating surface, the topography of annealed coatings is quite different from that of the as-deposited sample, as also AFM investigations have showed. Cross-section images of Ti-Si-B-N showed an inhomogeneous structure. The oxidation process promoted the formation of coarse crystallites on the surface, with amorphous-like region having fine crystallites at the bottom zone, followed by a uniform 200 nm thick layer composed by nano-crystallites and, finally, a darker bottom layer with nanostructured morphology. During the oxidation reaction, coarse Ti-oxide crystallites rapidly grew to 500 nm in size on the coating surface. SAED patterns showed that the coarse crystallites on the surface and in the amorphous-like region are composed by rutile-TiO_2 phase. The 800 nm-thick bottom layer exhibits a nano-crystalline morphology with average crystallite size of ~ 15 nm, and the SAED showed it to be made of TiB2 crystallites. Thus, as well as occurred at lower temperatures, the oxidation at 900°C induced the formation of a oxide layer on the coating surface, able to protect the coating from further oxidation. In addition, the thermal treatment at 900°C promoted the recrystallization of the TiO_2 and TiB_2 crystallites, at the bottom layer of the coating.

In the Ti-Al-Si-B-N coating, SAED indicated that the coarse crystallites on the coating surface and the crystallites beneath were constituted respectively by rutile-TiO_2 and corundum-Al_2O_3, formed as a consequence of Al outward diffusion to the surface [13,14]. These results are not fully consistent with other results reported in [7,9]. This is to be attributed to the different coating composition and the different thermal treatment conditions used in those works.

CONCLUSIONS

Ti-B-N, Ti-Si-B-N and Ti-Al-Si-B-N deposited on Si-[100] have been characterized in the as-deposited form and after air annealing at 700°C or 900°C for 4 hours.

Oxidation phenomena occurred in the Ti-B-N coating upon annealing at 700°C. The microstructure of the annealed coatings was mainly composed by a well-crystallized TiO_2 oxide. Si and Al+Si additions to the base Ti-B-N coating promoted the formation of an oxide layer able to protect these coatings from further oxygen diffusion at 700°C. The direct comparison of the two coatings showed that the Ti-Al-Si-B-N coating had a better oxidation resistance than the Ti-B-N and Ti-Si-B-N ones.

Upon annealing at 900°C, the Ti-Si-B-N coating showed a multilayered structure in which the bottom layer was not affected by oxidation, while the Ti-Al-Si-B-N coating was fully oxidized forming TiO_2 and Al_2O_3 oxide crystallites. The Si and Al+Si coatings were more oxidation-resistant than the base Ti-B-N coating.

REFERENCES

[1] D.V. Shtansky, Ph.V. Kiryukhantsev-Korneev, A.N. Sheveyko, A.E. Kutyrev, E.A. Levashov, A. Leyland, A.L. Yerokhin and A. Matthews, Surf. Coat. Technol., 200 (2005) 208.

[2] K. Yamamoto, S. Kujime, K. Takahara, Surf. Coat. Technol., 200 (2005) 1383.

[3] C.H. Zhang, X.C. Lu, H. Wang, J.B. Luo, Y.G. Shen, K.Y. Li, Applied Surface Science, 252 (2006) 6141.

[4] C.-T. Huang, J.-G. Duh, Surf. Coat. Technol., 81 (1996) 164.

[5] P.Steyer, D. Pilloud, J.F. Pierson,.,J.-P. Millet, M. Charnay, B. Stauder, P.Jacquot, Surf. Coat. Technol., 201 (2006) 4158.

[6] Ph.V. Kiryukhantsev-Korneev, D.V. Shtansky, M.I. Petrzhik, E.A. Levashov, and B.N. Mavrin, Surf. Coat. Technol., 201 (2007) 6143.

[7] A. Joshi, H.S. Hu, Surf. Coat. Technol., 76-77 (1995) 499.

[8] S. Inoue, H. Uchida, Y. Yoshinaga, K. Koterazawa, Thin Solid Films, 300 (1997) 171.

[9] C. Paternoster, A. Fabrizi, R. Cecchini, S. Spigarelli, Ph.V. Kiryukhantsev-Korneev, A. Sheveyko, Surf. Coat. Technol., 203 (2008) 736.

[10] F. Vaz, L. Rebouta, M. Andritschky, M.F. da Salva, J.C. Soares, Journal of the European Ceramics Society, 17 (1997) 1971.

[11 D. Pilloud, J.F. Pierso, M.C. Marco de Lucas, A. Cavaleiro, Surf. Coat. Technol., 202 (2008) 2413.

[12] A. Fabrizi, C. Paternoster, R. Cecchini, Ph.V. Kiryukhantsev-Korneev, A. Sheveyko, M. Cabibbo, M. Haidöpoulo, S. Spigarelli Materials Science Forum, 604-605 (2009) 19.

[13] S. Inoue, H. Uchida, Y. Yoshinaga, and K. Koterazawa, Thin Solid Films, 300 (1997) 171.

[14] M. Andritschky, F. Vaz, L. Rebouta, M.F. da Silva, and L.C. Soares, Surf. and Coat. Technol. 98 (1998) 912

Abstract

Comportamento ad ossidazione di rivestimenti nanostrutturati a base di Ti-B-N

Parole Chiave:
nanomateriali, ossidazione, rivestimenti, trattamenti termici, microscopia elettronica

I rivestimenti nanostrutturati a base Ti-B-N sono diffusamente utilizzati in varie applicazioni industriali per le loro spiccate proprietà meccaniche quali, elevata durezza, basso coefficiente di attrito, buona resistenza a corrosione. Quando a questi rivestimenti vengono aggiunti elementi, come ad esempio Al e Si, si registra un considerevole incremento nella resistenza a corrosione ed ossidazione. Nel presente lavoro sono stati studiati i rivestimenti Ti-B-N, Ti-Si-B-N e Ti-Al-Si-B-N, realizzati mediante sputtering magnetico assistito da impiantazione ionica (Ion Implantation Assisted Magnetron Sputtering - IIAMS). Lo studio della resistenza ad ossidazione è stato condotto sottoponendo il materiale (rivestimento su substrato di Si-[100] monocristallino) a 700 e 900°C per 4 ore in aria. Si è visto che il rivestimento più semplice, Ti-B-N, presenta fenomeni di ossidazione già a 700°C, mentre tale temperatura favorisce la formazione di stratificazione nei due rivestimenti Ti-Si-B-N e Ti-Al-Si-B-N. A 900°C il rivestimento Ti-Si-B-N ha mostrato miglior comportamento ad ossidazione rispetto ai Ti-B-N e Ti-Al-Si-B-N.